

Damping determination of FRP-confined reinforced concrete columns

Xiaoran Li, Yuanfeng Wang* and Li Su

Department of Civil Engineering, Beijing Jiaotong University, No.3 Shang Yuan Cun,
Hai Dian District, Beijing, China

(Received August 21, 2013, Revised January 2, 2014, Accepted May 23, 2014)

Abstract. Damping as a material property plays an important role in decreasing dynamic response of structures. However, very little is known about the evaluation and application of the actual damping of Fiber Reinforced Polymer Confined Reinforced Concrete (FRP-C RC) material which is widely adopted in civil engineering at present. This paper first proposes a stress-dependent damping model for FRP-C RC material using a validated Finite Element Model (FEM), then based on this damping-stress relation, an iterative scheme is developed for the computations of the non-linear damping and dynamic response of FRP-C RC columns at any given harmonic exciting frequency. Numerical results show that at resonance, a considerable increase of the loss factor of the FRP-C RC columns effectively reduces the dynamic response of the columns, and the columns with lower concrete strength, FRP volume ratio and axial compression ratio or higher longitudinal reinforcement ratio have stronger damping values, and can relatively reduce the resonant response.

Keywords: reinforced concrete columns; fiber reinforced polymers; energy dissipation; damping; finite element method; dynamic response

1. Introduction

Recently, the use of externally bonded FRP composites has become more widespread for the repair and retrofitting of concrete components. While the static behavior of the Fiber Reinforced Polymer Confined Reinforced Concrete (FRP-C RC) members has been extensively investigated, the studies on their dynamic behavior are still very few. Within these dynamic analysis works, the previous studies mainly focused on the pseudo-static capacity (Saadatmanesh *et al.* 1996, Seible 1997, Iacobucci 2003, Haroun and Elsanadedy 2005, Yalcin *et al.* 2008) modal parameter estimation based on free vibration testing (Jerome and Ross 1997, Capozucca and Nild 2002), and dynamic behavior with constant damping ratio (Zhu *et al.* 2006, Meftah *et al.* 2007). However, for the last part, the constant damping ratio cannot truly represent the complicated damping character in actual structures, because through extensive laboratory testing, damping displays a high degree of non-linearity. Unlike mass and stiffness, damping may not be an inherent characteristic of a dynamic system from the outset, and depends on many factors causing its obscure property. Therefore, the objective of this paper is to investigate this issue in FRP-C RC material.

We observe that in the non-linear zone, the hysteretic damping and the dissipating energy are both influenced by stress, strain, temperature, etc. (Lazan 1968) observed that damping displays a

*Corresponding author, MA, E-mail: cyfwang@bjtu.edu.cn

high non-linear behavior, and presented a relationship formula between the unit energy dissipation and stress amplitude of metal material. Soon afterwards, (Kume *et al.* 1982) transformed the relation of dissipating energy vs. maximum stress presented by (Lazan 1968), to a damping-stress diagram, and evaluated the loss factor of a cantilever beam for every known stress distribution. (Newmark and Hall 1969) also conducted a similar research on determining the damping, and gave approximately the same results as those given by (Lazan 1968) and (Kume *et al.* 1982). Following this idea, (Audenino and Calderale 1996, Audenino 1998, Audenino 2003) further developed these methods to identify that the material damping is not linear and depends on strain and strain rate, temperature, etc. (Audenino *et al.* 1996, Audenino *et al.* 2003) applied the least square exponential fitting method and autoregressive method to measure internal damping of highly stressed metals, and presented a relation of loss factor vs. strain amplitude for a metallic material. (Audenino *et al.* 2003) also proposed a theoretical relationship between temperature increment and metallic damping through thermo graphic analysis and specific damping measurement.

To date, most proposed methods to identify damping or describe damped dynamic behavior are based on viscous and hysteretic damping theories, whose mechanisms are well understood. And both viscous and hysteretic damping coefficients are generally constants which are suitable for describing damping properties in linear vibratory mechanical systems. However, they often contradict damping types in practice. The papers that deal with the dynamic behavior of structural members with non-linear damping are limited, and still remain to study the issues in metal and RC components. For example, an iterative numerical method was proposed by (Gounaris and Anifantis 1999, Gounaris *et al.* 2007) to calculate the loss factor of a cantilever steel beam until the damping of the previous iteration is nearly the same as that obtained in the last iteration. (Liu *et al.* 2005) obtained the non-linear correlation between loss factor and strain amplitude of high-damping alloy by experiment and applied it to the dynamics of elastic linkage mechanism. In addition, (Wen and Wang 2005) studied the vibration characteristics and dynamic response of concrete-filled steel tubular arch bridges under harmonic excitation with different damping ratios. (Wang and Li 2008) also applied a stress-related hysteretic damping model to study the dynamic response of a RC frame, and compared the numerical results to those computed by the viscous damping model. However, In fact, non-linear damping and its application in damping analysis for FRP-C RC material have not received enough attention. It is necessary to know the actual damping of FRP-C RC material and its application in civil engineering under various loads.

In this paper, the non-linear damping of FRP-C RC columns and its application in damping and dynamic response determination are numerically investigated. The hysteretic behavior of FRP-C RC columns with circular and rectangular sections is first simulated and validated against the cyclic test results of two FRP-C RC specimens. Then, using this validated Finite Element Model (FEM), the non-linear damping models of FRP-C RC material are presented by evaluations of the unit energy dissipation of FRP-C RC columns with different parameter combinations. Finally, based on these damping formulas, the damping and dynamic response of FRP-C RC columns at different harmonic exciting frequencies are calculated using an iterative method proposed by (Gounaris and Anifantis 1999, Gounaris *et al.* 2007) and parametric study is conducted to help to improve the understanding of the dynamic characteristics of FRP-C RC columns.

2. Loss factor computation

The damping model is widely used to model the energy dissipation in engineering. For this purpose, (Lazan 1968) proposed a measure of damping of a vibrating structure is the so-called loss factor, given by

$$\eta = \frac{W}{\pi \int_V \frac{\sigma^2}{E} dV} = \frac{W}{\pi k u_0^2} \quad (1)$$

where η is the loss factor, k is the stiffness of the system, u_0 is the displacement amplitude, σ is the stress amplitude, and W is the energy dissipation per cycle for the entire volume (V) of structure member, which can be denoted as

$$W = \int_V \Delta U(\sigma) dV = \pi c \omega u_0^2 \quad (2)$$

where ω is the exciting frequency, ΔU is the unit energy dissipation, and c is the damping coefficient. Substituting Eq. (2) into Eq. (1) deduces $c = \eta k / \omega$. The damping force is defined as $R = c \dot{u}$, where u is the harmonic displacement of the system and defined as $u = u_0 e^{i\omega t}$. Substituting $c = \eta k / \omega$ into the equation of the damping force reduces to the hysteretic damping force $R = i \eta k u$. Therefore, the loss factor is equal to the hysteretic damping coefficient. For these reasons, in order to evaluate the damping of FRP-C RC material, it is necessary to obtain the unit energy dissipation function $\Delta U(\sigma)$ of FRP-C RC members by hysteresis behavior modeling.

3. Hysteresis behavior modeling

It is well known that hysteretic damping affects structure's dynamic behavior, i.e. the more hysteretic energy dissipated, the better the specimen performs. The hysteretic dissipated energy refers to the absolute value of the summation of the enclosed areas in a lateral strength–displacement diagram. Therefore, the hysteretic behavior simulation of FRP-C RC columns is firstly conducted in the following section as required for the unit energy dissipation evaluation. An open source object-oriented non-linear structural analysis software, Open System for Earthquake Engineering Simulation (Open Sees), was used for the hysteretic behavior simulation of FRP-C RC columns.

3.1 Material models

An open source object-oriented non-linear structural analysis software, Open System for Earthquake Engineering Simulation (OpenSees), was used for the hysteretic behavior simulation of FRP-C RC columns. The cross-section of FRP-C RC element consists of confined concrete and steel reinforcement. Each component in the section was modeled with a different material model in OpenSees. The cross-section of FRP-C RC element consists of confined concrete and steel reinforcement. Each component in the section was modeled with a different material model in OpenSees. The constitutive models of Lam and Teng (Lam and Teng 2003, Lam and Teng 2003) were selected as the backbone curve for the concrete core material. The envelope curve of the models include three regions: parabolic ascending stress region, linear descending stress region, and constant residual stress region. The stress-strain relation for FRP-confined concrete proposed by (Lam and Teng 2003) is as follows:

Table 1 Property of column specimens

Source	Specimen designation	Axial load (kN)	L (mm)	Longitudinal reinforcement	f_{cu}' (MPa)	f_y (MPa)	Carbon-FRP composite properties		
							Tensile strength (MPa)	Tensile modulus (GPa)	Thickness (mm)
Yoneda <i>et al.</i> (2001)	TP-25	185	1350	12d16	30.0	374	4476	266	0.11
Ye <i>et al.</i> (2003)	CF30-4-48	492	600	8d16	25.8	358	3500	235	0.111

* L is the height of the lateral force action point from the bottom of the column;
 f_c' is the concrete compressive strength;
 f_y is the longitudinal reinforcement yield strength.

Table 2 Energy dissipation of the specimens at different drift ratios

Specimen name	Case study	Value				
TP-25	Drift ratio (Δ_i^a/L)	0.004	0.009	0.013	0.019	0.024
	Experimental results (kN×mm)	356.78	1612.36	2986.30	4569.21	6301.27
	Analytical results (kN×mm)	284.66	1381.61	2603.85	4341.91	5951.74
	Discrepancy (%)	20.21	14.31	12.8	4.97	5.55
CF30-4-48	Drift ratio (Δ_i/L)	0.008	0.015	0.024	0.033	0.040
	Experimental results (kN×mm)	286.75	905.18	1902.42	3244.13	4245.78
	Analytical results (kN×mm)	380.69	1043.09	1930.55	3080.12	4050.25
	Discrepancy (%)	32.76	15.23	14.8	5.06	4.61

* Δ_i is the maximum lateral displacement at the i th loop

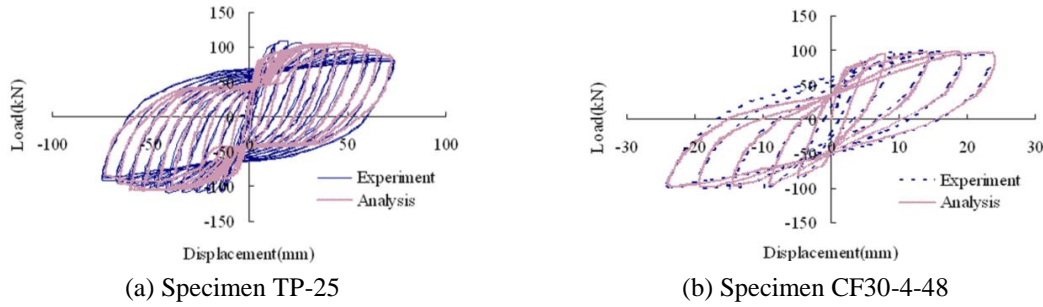


Fig. 1 Comparison of test data and numerical results for hysteretic response

$$\begin{cases} \sigma_c = E_c \varepsilon_c - \frac{(E_c - E_2)^2}{4f_{c0}'} \varepsilon_c^2 & 0 \leq \varepsilon_c \leq \varepsilon_t \\ \sigma_c = f_{c0}' + E_2 \varepsilon_c & \varepsilon_t \leq \varepsilon_c \leq \varepsilon_{cc} \end{cases} \quad (3)$$

where ε_t is the strain at the transition point of the parabolic portion to the linear portion in the stress-strain relation curve, defined as

$$\varepsilon_t = 2f_{c0}' / (E_c - (f_{cc}' - f_{c0}') / \varepsilon_{cc}) \quad (4)$$

where E_c is the elastic modulus of unconfined concrete, f_{cc}' and ε_{cc} are the compressive strength and corresponding strain of the confined concrete, respectively, and can be denoted as the following:

$$f_{cc}' = f_{c0}' + 3.3f_{c0}'(f_1 / f_{c0}') \quad (5)$$

$$\varepsilon_{cc} = \varepsilon_{c0}' \cdot (1.75 + 12(f_1 / f_{c0}')(\varepsilon_{h,rupt} / \varepsilon_{cc})^{0.45}) \quad (6)$$

where f_{c0}' and ε_{c0}' are the compressive strength and corresponding strain of the unconfined concrete, respectively, $\varepsilon_{h,rupt}$ is the FRP hoop strain at rupture, selected as $0.586\varepsilon_f$ for carbon-FRP (Lam and Teng 2003) in this study, ε_f is the FRP material ultimate tensile strain, and f_1 is the actual maximum confining pressure, defined as $f_1 = 2 E_f t_f \varepsilon_{h,rupt} / D$, where E_f and t_f are the elastic modulus and thickness of the FRP, respectively, and D is the diameter of the concrete core.

For the FRP-C RC columns with rectangular section, the only modification required is the confining pressure (Lam and Teng 2003), given by

$$f_{1r} = \frac{b}{h} \frac{1 - (((b/h)(h - 2R_c)^2 + (h/b)(b - 2R_c)^2) / (3A_g)) - \rho}{1 - \rho} \cdot \frac{2E_f t_f \varepsilon_f}{\sqrt{h^2 + b^2}} \quad (7)$$

where b and h are the width and depth of the cross section, R_c is the corner radius of the cross section, ρ is the longitudinal reinforcement ratio, and A_g is the sectional area.

The constitutive models described above were cast into the concrete model of Kent-Park (Taucer *et al.* 1991) modified by (Scott *et al.* 1982), which is built into Open Sees with hysteretic features. The hysteretic behavior of the steel reinforcement in the FRP-C RC columns can be simulated using the non-linear constitutive model of Giuffre-Menegotto-Pinto (Filippou *et al.* 1983). The elastic and yield asymptotes in this model are assumed to be straight lines, and the unloading slope remains constant and equals to the initial slope. More details about the definition of cyclic parameters can be found in reference (Filippou *et al.* 1983).

4. Calculation of the unit energy dissipation of FRP-C RC columns

To evaluate the damping of FRP-C-RC material, the FRP-C RC columns experimentally investigated by (Tao and Yu 2006, Lam and Teng 2003) were taken as numerical models. The basic geometrical and material properties are shown in Table 3.

Table 4 shows the other parameters selected in the analysis, three values were selected in the practical range for each parameter, and only one parameter at a time was considered as a variable.

Because the models of Lam and Teng (Lam and Teng 2003, Lam and Teng 2003) are for the sufficient confinement case (the actual confinement ratio is $f_1/f_{c0}' \geq 0.07$ or $f_{1r}/f_{c0}' \geq 0.07$), all case studies used in this paper were in this range. Using the above numerical method, the hysteretic curves and energy dissipation at different stress amplitudes of these columns were evaluated in different parameter combinations.

The unit energy dissipation of the columns was calculated as the product of the column base shear load and head displacement at the i th loop divided by the entire volume of the column. The

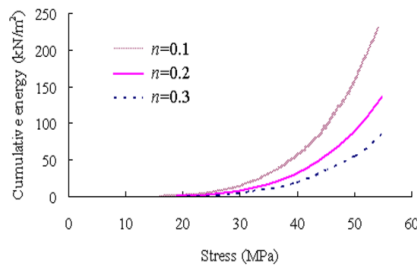
Table 3 Properties of column specimens

Source	L (mm)	b (mm)	h (mm)	D (mm)	Longitudinal reinforcement	Stirrup	FRP Composite properties		
							ε_f (MPa)	E_f (GPa)	t_f (mm)
Tao and Yu (2006)	1500			150	6 Φ 12	6@150	4212	255	0.17
Lam and Teng (2003b)	600	200	200		4 Φ 12	6@200	4519	257	0.165

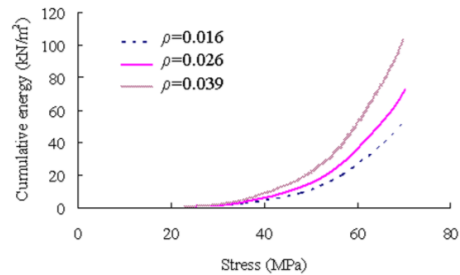
Table 4 Case study parameter matrix

Parameters	Case 1	Case 2	Case 3	
FRP volume ratio (γ)	Circular section	0.005 (1 layer)	0.009(2 layer)	0.014 (3 layer)
	Rectangular section	0.003 (1 layer)	0.010(3 layer)	0.016 (5 layer)
Longitudinal reinforce ment ratio (ρ)	Circular section	0.027 ($d = 10$ mm)	0.052 ($d = 14$ mm)	0.086 ($d = 18$ mm)
	Rectangular section	0.016 ($d = 14$ mm)	0.026 ($d = 18$ mm)	0.039 ($d = 22$ mm)
Axial compression ratio (n) (circular and rectangular section)	0.1	0.2	0.3	
Concrete strength(MPa)(f_{cu}') (circular and rectangular section)	30	40	50	

* d is the diameter of the longitudinal reinforcement



(a) Effect of axial compression ratio($f_{cu}' = 30$ MPa, $\rho = 0.039$, $\gamma = 0.016$)



(b) Effect of longitudinal reinforcement ratio($f_{cu}' = 50$ MPa, $n = 0.1$, $\gamma = 0.016$)

Fig. 2 The relation between the unit energy dissipation and maximum stress of the rectangular FRP-C RC columns

stress amplitude was obtained by extracting the calculation result of cross section at column base.

It was found that at the same stress amplitude, the unit energy dissipation decreases with the increase of the axial compression ratio ($n = N/(f_{c0}'A)$, where N is the axial load, A is the gross area of the column's section.) and f_{c0}' is the concrete compression strength. It was also found that both energy dissipation at every loop and the maximum energy dissipation become bigger with the increase of the longitudinal reinforcement ratio, and the difference among the curves enlarge gradually with the increase of stress amplitude. To limit the size of this paper, the effects of the axial compression ratio and reinforcement ratio on the unit energy dissipation of the FRP-C RC columns with rectangular section are only plotted in Fig. 2. For example, at a stress of 30.4 MPa, the unit energy dissipation values of columns with the axial compression ratios equal to 0.1 and 0.3 are 16.06 kN/m² and 7.16 kN/m², respectively, and reach 154.98 kN/m² and 55.39 kN/m² at a

stress of 49.71 MPa. The columns with different concrete strengths show the same law. For the columns with the longitudinal reinforcement ratios equal to 0.016 and 0.039, at a stress of 47.71 MPa, the unit energy dissipation values are 9.07 kN/m² and 19.74 kN/m², and at the maximum stress, the unit energy dissipation reaches 52.78 kN/m² and 103.21 kN/m², respectively. Through the calculation, we also found that the FRP volume ratio ($\gamma = 4 t_f / D$, for circular section, $\gamma = 2 t_f (h_2 + b_2) / h_2 b_2$, for rectangular section) turns out to be a sensitive parameter affecting the maximum energy dissipation when the limit strain of concrete at the column base occurs. For instance, the maximum unit energy dissipation value of the rectangular column with the FRP volume ratio equal to 0.003 is 20.96 kN/m², which is only about 9.1% of the result calculated with $\gamma=0.016$. The results is possibly attributed to that the increase of the axial compression ratio will reduce the horizontal displacement, the concrete with lower strength will form more plastic deformation and micro-fracture development, and the increase of the FRP volume ratio and reinforcement ratio will result in larger ductility.

5. The unit energy dissipation formulation of FRP-C RC columns

To quantitatively evaluate the loss factor and readily apply it to the FEA for the simulation of the dynamic behavior of FRP-C RC columns, as stated in the Eq. (1), the establishment of the unit energy dissipation formula of the FRP-C RC material is required. Only the stress amplitude at a time was considered as a variable, the unit energy dissipation is in agreement with the formula form $\Delta U(\sigma) = J \cdot \sigma^n$, stated by (Lazan 1968), where J and n are material constants. The relevant formula for single parameter and material constants can be regressed by SPSS program one by one until achieve a unified expression by combining these formulas. Through the parametric study of the energy dissipation in Section 4, the next five non-linear regression equations of unit energy dissipation of FRP-C RC columns were established considering different concrete strength, axial compression ratio, longitudinal reinforcement ratio and FRP volume ratio in reasonable value range.

For circular section:

$$\Delta U(\sigma, \rho, \gamma, n, f_{cu}') = 2471.341 \cdot \sigma^{3.72} \cdot (1 + \rho)^{8.757} \cdot (1 + \gamma)^{-35.64} \cdot (1 + f_{cu}')^{-3.969} \cdot (1 - 2.455n + 2.86n^2) \quad (8)$$

For rectangular section:

$$\Delta U(\sigma, \rho, \gamma, n, f_{cu}') = 1815.667 \cdot \sigma^{4.609} \cdot (1 + \rho)^{30.116} \cdot (1 + \gamma)^{-35.64} \cdot (1 + f_{cu}')^{-3.969} \cdot (1 - 4.576n + 6.499n^2) \quad (9)$$

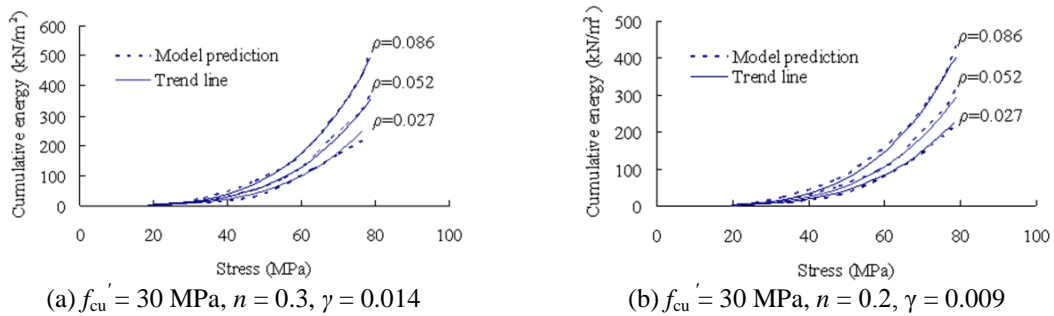


Fig. 3 Comparison of the model prediction and regression results for circular columns

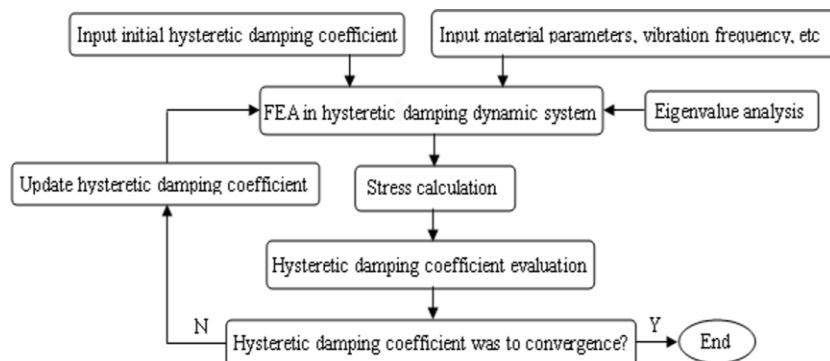


Fig. 4 The iterative scheme for the hysteretic damping coefficient computation

The R^2 values of the regression results, for circular section given by Eq. (8) and for rectangular section given by Eq. (9), are 0.992 and 0.987 respectively. To limit the size of the regression results matrix, only two cases of the predicted response are compared to the regression results for the circular FRP-C RC columns, as shown in Fig. 3. Excellent correlation was obtained for the energy-stress relationships in both the circular and rectangular columns.

6. Iterative computation of hysteretic damping coefficient and dynamic response of the FRP-C RC columns

It is well known that material damping affects the dynamic behavior of structures, and the damping also depends on the stress distribution in structures, as depicted in previous sections. Since damping and stress are tightly coupled, a successive iteration method proposed by (Gounaris and Anifantis 1999, Gounaris *et al.* 2007) is used here to study the damping and dynamic response developed in the FRP-C RC columns, especially in the resonance zone where high-amplitude vibrations are induced and can cause maximum stress and severe damage.

6.1 Material models

It is well known that material damping affects the dynamic behavior of structures, and the damping also depends on the stress distribution in structures, as depicted in previous sections. Since damping and stress are tightly coupled, a successive iteration method proposed by (Gounaris and Anifantis 1999, Gounaris *et al.* 2007) is used here to study the damping and dynamic response developed in the FRP-C RC columns, especially in the resonance zone where high-amplitude vibrations are induced and can cause maximum stress and severe damage.

6.2 Numerical results and discussion

In this section, to apply the above iterative method to FRP-C RC material, a cantilever FRP-C RC columns of 300 mm in diameter by 2000 mm in height, and cantilever FRP-C RC columns of 150×150 mm in cross-section by 600 mm in height were considered. Discretized columns were approached by 20 elements of equal length and 42 nodes. The calculation of the loss factor using Eq. (11) or (12) starts by assuming an initial loss factor of 0.01. The dynamic responses of these

columns are obtained by solving Eqs. (15) and (16) for a number of harmonic frequencies at constant amplitudes of excitation force 8 kN.

The evaluated loss factors and maximum stress values for the circular columns excited at 50 rad/s ~ 390 rad/s are plotted in Figs. 5-6, and a parametric study is carried out to better understand the dynamic behavior of FRP-C RC columns at the resonance. As expected, the peak value of the loss factor obtained with Eq. (11) is located at the resonance frequency, and the maximum stress at the fixed end of the column also occurs at the fundamental natural frequency. The maximum loss factor increases with the decrease of concrete strength, FRP volume ratio and axial compression ratio. The higher the reinforcement ratio, the larger the loss factor. And the presence of high damping decreases maximum stress at resonance. As shown in these figures, when $f_{cu}' = 30$ MPa, the maximum loss factor calculated with Eq. (11) is 0.15, and reduces to 0.09 with $f_{cu}' = 50$ MPa. The corresponding stress amplitude evaluated by the FEM is 42.72 MPa with $f_{cu}' = 30$ MPa, which accounts for about 60.26% of the result when $f_{cu}' = 50$ MPa. The columns with different FRP volume ratio and axial compression ratio show the same law. For the columns with the longitudinal reinforcement ratios equal to 0.027 and 0.086, at resonance, the loss factors are 0.11 and 0.13, and the maximum stresses are 61.49 MPa and 51.22 MPa, respectively. These results may be due to that the evaluation of the loss factor of the FRP-C RC columns related with the parameters from Table 4 inside the elements in the FEM.

The rectangular columns show the same law. However, due to space constraints, the corresponding diagrams are not shown here. Since the present study focuses on the dynamic responses at resonance, Table 5 shows the loss factor and dynamic responses of the rectangular FRP-C RC columns with different parameters at the resonance frequency.

Fig. 7 shows comparisons between the displacements of the FRP-C RC columns obtained by Eqs. (11) and (12) and those obtained by constant loss factors 0.03, 0.04, 0.05, 0.06 and 0.08. We observed that the peak value of the displacement was located at the position of the frequencies near resonance, and the maximum displacement values obtained by Eqs. (11) and (12) were 0.019 m and 0.034 m, respectively, which were only about 29.69% and 25.0% of the results obtained with the constant loss factors $\eta = 0.03$ and $\eta = 0.04$. By the finite element approach, we also found that the maximum stress values evaluated by Eqs. (11) and (12) were 79.16 MPa and 102.51 MPa, respectively, which were also considerably lower than those evaluated with the constant loss factors. This may be attributed to the fact that the hysteretic damping coefficients of the FRP-C RC columns clearly increase as reaching the resonant frequency, and this behavior can effectively reduce the displacement and stress amplitude near the resonant frequency.

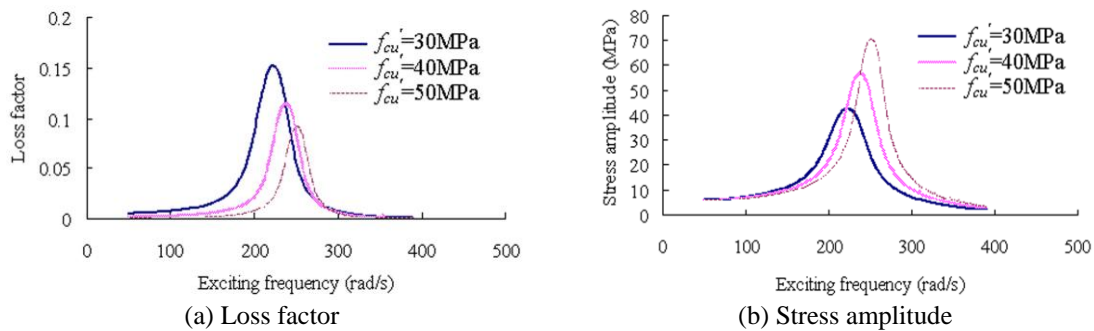


Fig. 5 Effect of concrete strength ($n=0.1$, $\gamma = 0.014$, $\rho = 0.052$)

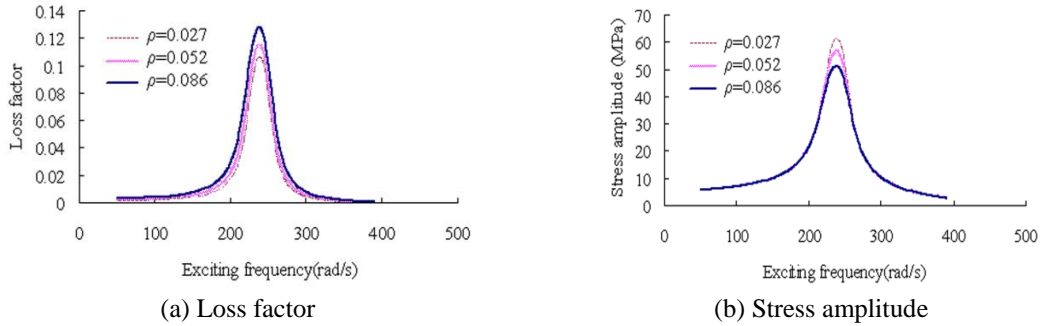
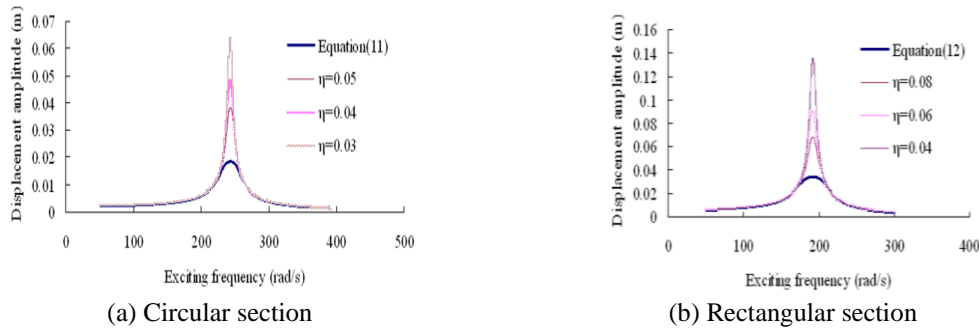
Fig. 6 Effect of longitudinal reinforcement ratio ($n = 0.1$, $\gamma = 0.014$, $f'_{cu} = 40\text{MPa}$)

Fig. 7 Computed maximum displacement for FRP-C RC column

Table 5 Loss factors and dynamic responses of rectangular FRP-C RC columns with different parameters at resonance

Parameters	Base values of other parameters	Case study parameter matrix	Maximum loss factor	Maximum displacement (m) ^a	Maximum stress (MPa) ^b
f'_{cu} (MPa)	$\rho = 0.016$, $n = 0.3$, $\gamma = 0.010$	30	0.184	0.029	70.06
		40	0.141	0.033	92.10
		50	0.114	0.037	114.0
γ	$f'_{cu} = 40\text{Ma}$, $\rho = 0.016$, $n = 0.3$	0.003	0.147	0.032	88.13
		0.010	0.141	0.033	92.10
		0.016	0.135	0.034	96.42
ρ	$f'_{cu} = 40\text{ MPa}$, $\gamma = 0.010$, $n = 0.3$	0.016	0.141	0.033	92.10
		0.026	0.153	0.030	84.69
		0.039	0.169	0.027	76.38
n	$f'_{cu} = 40\text{ MPa}$, $\gamma = 0.010$, $\rho = 0.016$	0.1	0.188	0.025	68.73
		0.2	0.161	0.029	80.46
		0.3	0.141	0.033	92.10

near resonance, and the maximum displacement values obtained by Eqs. (11) and (12) were 0.019 m and 0.034 m, respectively, which were only about 29.69% and 25.0% of the results obtained with the constant loss factors $\eta = 0.03$ and $\eta = 0.04$. By the finite element approach, we also found that the maximum stress values evaluated by Eqs. (11) and (12) were 79.16 MPa and 102.51 MPa, respectively, which were also considerably lower than those evaluated with the constant loss factors. This may be attributed to the fact that the hysteretic damping coefficients of the FRP-C RC

columns clearly increase as reaching the resonant frequency, and this behavior can effectively reduce the displacement and stress amplitude near the resonant frequency.

7. Conclusions

The non-linear damping models of the FRP-C RC circular and rectangular columns were established by considering different concrete strength, axial compression ratio, longitudinal reinforcement ratio and FRP volume ratio in reasonable value range. Based on the proposed damping-stress relations, an iterative numerical method proposed by (Gounaris *et al.* 1999 and Gounaris *et al.* 2007) is used here for the computation of the hysteretic damping coefficient and actual dynamic response for FRP-C RC columns. The following conclusions can be drawn:

(1) By comparing cyclic numerical results to those reported by other researchers, the correctness of the proposed model for simulating the hysteretic behavior of FRP-C RC columns was validated, which is required for the establishment of non-linear damping model of FRP-C RC material.

(2) By applying the proposed iterative computation, it is found that the maximum loss factor and dynamic response of the FRP-C RC columns are located at the resonance, and considerably lower than those evaluated by constant loss factors.

(3) Near the resonant frequency, the loss factors of FRP-C RC columns increase with the decrease of concrete strength, FRP volume ratio and axial compression ratio. And the higher the longitudinal reinforcement ratio, the larger the loss factor. Moreover, the presence of high loss factor reduces the dynamic response of the columns at resonance.

Acknowledgments

The authors would like to acknowledge the financial support from National Natural Science Foundation of China, under grant No. 51278038 .

References

- Saadatmanesh, H., Ehsani, M.R. and Jin, L. (1996), "Seismic strengthening of circular bridge pier models with fiber composites", *ACI Struct. J.*, **93**(6), 639-647.
- Seible, F., Priestley, M.J.N., Hegemier, G.A. and Innamorato, D. (1997), "Seismic retrofit of RC columns with continuous carbon fiber jackets", *J. Compos. Constr.*, **1**(2), 52-62.
- Iacobucci, R.D., Sheikh, S.A. and Bayrak, O. (2003), "Retrofit of square concrete columns with carbon fiber-reinforced polymer for seismic resistance", *ACI Struct. J.*, **100**(6), 785-794.
- Haroun, M.A. and Elsanadedy, H.M. (2005), "Behavior of cyclically loaded squat reinforced concrete bridge columns upgraded with advanced composite-material jackets", *J. Bridge. Eng.*, **10**(6), 741-748.
- Yalcin, C., Kaya, O. and Sinangil, M. (2008), "Seismic retrofitting of RC columns having plain bars using CFRP sheets for improved strength and ductility", *Constr. Build. Mater.*, **22**(3), 295-307.
- Jerome, D.M. and Ross, C.A. (1997), "Simulation of the dynamic response of concrete beams externally reinforced with carbon-fiber reinforced plastic", *Comput. Struct.*, **64**(5/6), 1129-1153.
- Capozucca, R., and Nild, Cerri, M. (2002), "Static and dynamic behavior of RC beam model strengthened by CFRP-sheets", *Constr. Build. Mater.*, **16**(2), 91-99.

- Zhu, Z.Y., Ahmad, I. and Mirmiran, A. (2006), "Fiber element modeling for seismic performance of bridge columns made of concrete-filled FRP tubes", *Eng. Struct.*, **28**, 2023-2035.
- Meftah, S. A., Yeghneem, R., Tounsi, A. and Adda, bedia, E.A. (2007), "Seismic behavior of RC coupled shear walls repaired with CFRP laminates having variable fibers spacing", *Constr. Build. Mater.*, **21**, 1661-1671.
- Lazan, B.J. (1982), "Damping of material and members in structural mechanics", *Pergamon press*, London. (1968)
- Kume, Y., Hashimoto, F. and Maeda, S. (1982), "Material damping of cantilever beams", *J. Sound. Vib.*, **80**(1), 1-10.
- Newmark, N.M. and Hall, W.J. (1969), "Seismic design criteria for nuclear reactor facilities", *Proceeding of the 4th International Conference on Earthquake Engineering*, Santiago, Chile, 37-50.
- Audenino, A.L. and Calderale, P.M. (1996), "Measurement of non-linear internal damping in metals: processing of decay signals in a uniaxial stress field." *J. Sound. Vib.*, **198**(4), 395-409.
- Audenino, A.L., Zanetti, E.M. and Calderale, P.M. (1998), "Assessment of internal damping in uniaxially stressed metals: exponential and autoregressive methods", *J. Dyn. Syst. Meas. Contr.*, **120**(2), 177-184.
- Audenino, A.L., Crupi, V. and Zanetti, E.M. (2003), "Correlation between thermography and internal damping in metals", *Int. J. Fatigue.*, **25**, 343-351.
- Goumaris, G.D. and Anifantis, N.K. (1999), "Structural damping determination by finite element approach", *Comput. Struct.*, **73**, 445-452.
- Goumaris, G.D., Antonakakis, E. and Papadopoulos, C.A. (2007), "Hysteretic damping of structures vibrating at resonance: An iterative complex eigensolution method based on damping-stress relation", *Comput. Struct.*, **85**, 1858-1868.
- Liu, H.Z., Wang, J.P., Zhang, Z.M., Yuan, D.N. and Liu, L.L. (2005), "Strain-dependent nonlinear damping and application to dynamic analysis of elastic linkage mechanism", *J. Sound. Vib.*, **281**, 399-408.
- Wen, J. and Wang, Y.F. (2005), "The influence of damping change on dynamic response of concrete-filled steel tubular arch bridges", *Proceeding of the 4th Int. Conference on Advances in Steel Structures*, Shanghai, China.
- Wang, Y.F. and Li, P. (2008), "Analysis of influence of material damping on the dynamic response of reinforced concrete frame structures", *China. Civil Eng. J.*, **41**(11), 39-43.
- Lam, L. and Teng, J.G. (2003), "Design-oriented stress-strain model for FRP-confined concrete", *Constr. Build. Mater.*, **17**, 471-489.
- Lam, L. and Teng, J.G. (2003), "Design-oriented stress-strain model for FRP-confined concrete in rectangular columns", *J. Reinf. Plast. Comp.*, **22**(13), 1149-1186.
- Taucer, F.F., Spaone, E. and Filippou, F.C. (1991), "A fiber beam-column element for seismic response analysis of reinforced concrete structures", Earthquake Engineering Research Center, University of California, Berkeley.
- Scott, B.D., Park, R. and Priestley, M. (1982), "Stress-strain behavior of concrete confined by overlapping hoops at low and high strain rates", *ACI J.*, **79**(1), 13-27.
- Filippou, F.C., Popov, E.P. and Bertero, V.V. (1983), "Effects of bond deterioration on hysteretic behavior of reinforced concrete joints", *Earthq. Eng. Res. Center*, University of California, Berkeley.
- Yoneda, K., Kawashima, K. and Shoji, G. (2001), "Seismic retrofit of circular reinforced bridge columns by wrapping of carbon fiber sheets", *J. Struct. Mech. Earthq. Eng.*, **682**, 41-56.
- Ye, L.P., Zhang, K., Zhao, S.H. and Feng, P. (2003), "Experimental study on seismic strengthening of RC columns with wrapped CFRP sheets", *Constr. Build. Mater.*, **17**, 499-506.
- Tao, Z. and Yu, Q. (2006), "New type composite structure column-the experiment, theory and methods", *Science press*, Beijing, 317-351.